Catal Lett (2012) 142:1061–1066
DOI 10.1007/s10562-012-0877-2

# Bimetallic FeCo Nanocrystals Supported on Highly Porous Silica Aerogels as Fischer–Tropsch Catalysts

**Danilo Loche · Maria F. Casula · Anna Corrias · Sergio Marras · Pietro Moggi**

Received: 8 May 2012 / Accepted: 15 July 2012 / Published online: 31 July 2012
© Springer Science+Business Media, LLC 2012

**Abstract** In this work, nanocomposites constituted of FeCo alloy nanoparticles dispersed on a highly porous silica aerogel have been designed as catalysts for low temperature Fischer–Tropsch synthesis. The catalysts were characterized by XRD, TEM, $N_2$ physisorption and SEM analysis. A high catalytic activity with CO conversions up to 95 % has been obtained, with enhanced selectivity for the $C_2$–$C_4$ hydrocarbons.

**Keywords** Alloy · Nanocomposite · Aerogel · Fischer–Tropsch

## 1 Introduction

The Fischer–Tropsch (FT) synthesis represents a versatile route for the production of liquid hydrocarbons starting from different feedstocks (natural gas, syngas, biosyngas, coal, waste) which has obtained renewed attention as a way to develop the technology behind the clean production of renewable transportation fuels [1, 2]. The catalyst type represents a key parameter which impacts the design of the FT process in terms of the reaction feed, temperature, product quality and yield; to name a few Fe, Co, Ni and Ru are the most used metal catalysts in the low temperature FT synthesis, where Fe and Co are the most attractive on the industrial scale as they combine the best activity to their limited cost [3–5]. It has been proven that by using both Fe and Co (either in the form of alloy or in the form of the oxide precursors without any reduction pre-treatment) the activity and selectivity over the product spectrum can be improved compared to single metal catalysts, with particular reference to an increase in the formation of products rich in olefins [6–8]. The FeCo catalysts seem to be interesting in the technologies related to the use of low $H_2$:CO ratios (<2) and high level of $CO_2$, i.e. those that make use of biosyngas (BTL, biomass to liquid) [9] or syngas from coal (CTL, coal to liquid), taking advantage of the good activity of the Fe through the water gas shift reaction ($CO + H_2O \leftrightarrow CO_2 + H_2$).

Improved catalytic activity is obtained by making use of metals loaded on suitable supports [10], such as $SiO_2$, $Al_2O_3$ and $TiO_2$ matrices prepared by sol–gel routes. In particular, aerogel catalysts produced by special drying techniques, such as supercritical drying which ensure the preservation of the pore architecture of the original gel, have been shown to be more effective than the corresponding xerogels, obtained by conventional drying, as well as ordered mesoporous materials [11–14].

Recent advances in the design of aerogels has led to the controlled production of nanocomposites made out of catalytically-active nanoparticles dispersed on highly porous supports [15], which have been successfully applied in heterogeneous catalysis [16, 17]. Preliminary results on

---

**Electronic supplementary material** The online version of this article (doi:10.1007/s10562-012-0877-2) contains supplementary material, which is available to authorized users.

D. Loche (✉) · M. F. Casula · A. Corrias
Dipartimento di Scienze Chimiche e Geologiche and INSTM,
Università di Cagliari, S.P. Monserrato-Sestu Km 0.700,
09042 Cagliari, Monserrato, Italy
e-mail: daniloche@unica.it

*Present Address:*
S. Marras
Istituto Italiano di Tecnologia, via Morego 30,
16163 Genoa, Italy

P. Moggi
Dipartimento di Chimica Organica e Industriale, Università di
Parma, Parco Area delle Scienze 17/A, 43100 Parma, Italy

silica-supported nanocomposite aerogels as FT catalysts have suggested the potential of these materials which can be ascribed to the unique properties of aerogels such as high surface area, large pore volume and low density [18]. In particular, it is expected that the high active surface and the 3D interconnected pore network may favour mass transport and the passage of a higher fraction of products [18].

In this work, FeCo–$SiO_2$ nanocomposites in which an iron–cobalt equimolar nanocrystalline alloy is finely dispersed on a highly porous silica aerogel matrix were prepared as prospective catalysts for the Fischer–Tropsch reaction. High CO conversion, elevated selectivity towards light fractions and relatively low reaction temperatures suggest that FeCo–$SiO_2$ aerogels can be good candidates for the design of Fischer–Tropsch catalysts without the need of adding promoters.

## 2 Experimental Section

### 2.1 Synthesis of FeCo–$SiO_2$ Aerogel Catalysts

FeCo–$SiO_2$ aerogel catalysts were prepared according to a previously reported sol–gel procedure based on co-gelation of the silica and alloy precursors [19], followed by high temperature supercritical drying and thermal treatments. An equimolar FeCo alloy was prepared, and the overall alloy loading in the nanocomposite was either 5 or 10 wt%.

Briefly, the preparation route makes use of tetraethoxysilane ($Si(OC_2H_5)_4$, Aldrich 98 %, TEOS) and iron (III) and cobalt (II) nitrates ($Fe(NO_3)_3{\cdot}9H_2O$, Aldrich, 98 %, and $Co(NO_3)_2{\cdot}6H_2O$, Aldrich, 98 %) as precursors for the silica matrix and for the FeCo alloy, respectively, and of absolute ethanol (Fluka) as mutual solvent. The sol–gel procedure includes an acidic pre-hydrolysis of TEOS and of the metal salts, followed by the addition of urea ($NH_2CONH_2$, Sigma-Aldrich, >99.0 %) as a gelation promoter under reflux for 2 h. The viscous sol is poured into a closed container and kept at 40 °C until gelation, which occurs in less than 2 days. Table 1 summarizes the amounts used for the preparation of the aerogel which exhibited the best catalytic results, i.e. the FeCo–$SiO_2$ nanocomposite having an overall metal loading of 10 wt% and an equimolar alloy composition.

To obtain the aerogel catalysts, supercritical drying of the gels in an autoclave (Parr, 300 $cm^3$) was performed. The autoclave was filled with an appropriate amount of ethanol and flushed with $N_2$ before being closed and heated up until 330 °C and 70 atm were reached. Finally, the autoclave was vented down to atmospheric pressure and cooled to room temperature.

The aerogels obtained by this route are extremely lightweight, with typical values of apparent density of 0.07 g $cm^{-3}$, and were powdered and calcined at 450 °C in static air for 1 h in order to eliminate the reaction by-products. The samples were finally reduced at 800 °C in $H_2$ flow to ensure the formation of the alloy phase.

### 2.2 Characterization of FeCo–$SiO_2$ Aerogel Catalysts

Wide-angle X-ray diffraction (XRD) patterns were recorded on a Panalytical Empyrean diffractometer equipped with a graphite monochromator on the diffracted beam and an X'Celerator linear detector. The scans were collected within the range of 10°–90° ($2\theta$) using Cu K$\alpha$ radiation.

Transmission electron microscopy (TEM) bright field (BF) images were obtained on a JEOL 200CX microscope equipped with a tungsten cathode operating at 200 kV. Prior to observation, the powdered samples were deposited on carbon-coated copper grids.

Scanning electron microscopy (SEM) images were obtained using a Philips XL-30 CP microscope equipped with an RBS detector for the back-scattered electrons and an EDS analyzer to investigate the surface elemental composition of catalysts.

Nitrogen adsorption isotherms were measured on a Fisons Instruments Sorptomatic 1990 system at 196 °C on samples degassed at 200 °C in a vacuum better than $10^{-1}$ Pa for 12 h.

### 2.3 Catalytic Apparatus and Fischer–Tropsch Synthesis Conditions

Reaction tests were performed in a stainless-steel tubular reactor especially designed for FT synthesis with an inner diameter of 10 mm, heated by an electric resistance and thermally insulated with glass wool.

The inlet and outlet gases (CO, $CO_2$ and hydrocarbons with $C_n \leq 4$, where n is an integer related to the hydrocarbon chain length) were analyzed by a Dani 3400

**Table 1** Experimental details for the preparation of about 2 g of the FeCo–$SiO_2$ nanocomposite aerogel having a 10 wt% loading of the metal phase

| Sample | Fe precursor (g) | Co precursor (g) | $SiO_2$ precursor (mL) | $Time_{gel}$ (h) |
|---|---|---|---|---|
| FeCo–$SiO_2$ | 0.8323 | 0.5995 | 7.9 | 42 |

gas-chromatograph equipped with a TCD detector, whereas for hydrocarbons with $C_n \geq 7$ a Dani 87.40 HT gas-chromatograph with a capillary column and FID detector was used. Condensable hydrocarbons were collected by condensation and were the average product of the whole run (usually 4 days) at constant reaction conditions. The hydrocarbons with $C_n$ 5 and 6 were calculated by extrapolation of experimental data using the Anderson-Schulz-Flory function [20].

In a typical experiment, 5 g of catalyst, diluted with 5 g of commercial silica (Aldrich), were preheated in flowing $H_2$ until the reaction temperature (at the reaction pressure of 20 bar) was reached.

The reaction was carried out with a mixture of CO and $H_2$ with a total flow rate of 15 L/h, $H_2$:CO ratio of the inlet mixture of either 2:1 or 1.5:1 and temperature range 180–220 °C.

## 3 Results and Discussion

Figure 1 compares the X-ray diffraction patterns of the aerogel samples as obtained after the supercritical drying procedure and after the reduction treatment at 800 °C under $H_2$ flow. In the aerogel samples prior to thermal treatment X-ray diffraction shows the presence of the typical halos due to amorphous silica. In addition, in the 10 wt% sample extra broad and weak peaks due to two separate nanocrystalline phases of iron (III) and cobalt (II), namely the iron oxyhydroxide ferrihydrite, and a layered cobalt silicate hydroxide are present [22]. After the reduction treatment the only peaks superimposed to the silica halos can be ascribed to the iron–cobalt alloy which has a body cubic centered structure, indicating a complete reduction of the dispersed phase. In particular, the peaks are more evident in the 10 wt% sample as a consequence of both a higher loading of the dispersed phase and a larger average nanocrystalline size. The average nanocrystal size as derived from line broadening is 4.2 and 9.1 nm for the 5 and 10 wt% nanocomposites, respectively. The formation of the FeCo alloy, which cannot be deduced unambiguously from XRD data due to the similarity with the pure bcc-Fe structure, was further confirmed by X-ray absorption spectroscopy [23].

SEM investigation, as shown in the representative image reported in Fig. 2, confirms that Fe and Co are in equimolar amounts.

Figure 3 shows representative TEM images of the FeCo–$SiO_2$ aerogel nanocomposites as obtained after the reduction treatment. The nanocrystalline alloy phase is homogeneously dispersed throughout the silica matrix: in particular, in agreement with XRD data, the nanocrystal size increases with the alloy loading from 4 to 10 nm. TEM

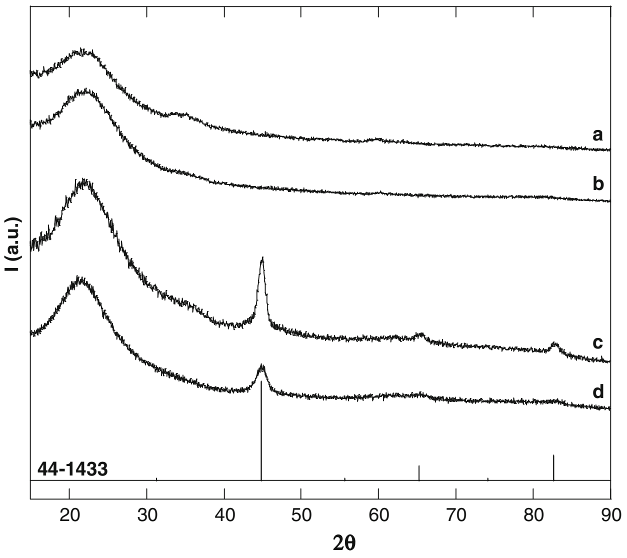

**Fig. 1** XRD patterns for the aerogel nanocomposites as obtained and after the reduction treatment with an overall alloy loading of 10 wt% (*curves a* and *c*) and 5 wt% (*curves b* and *d*) respectively, and corresponding FeCo alloy reference PDF-2 card [21]

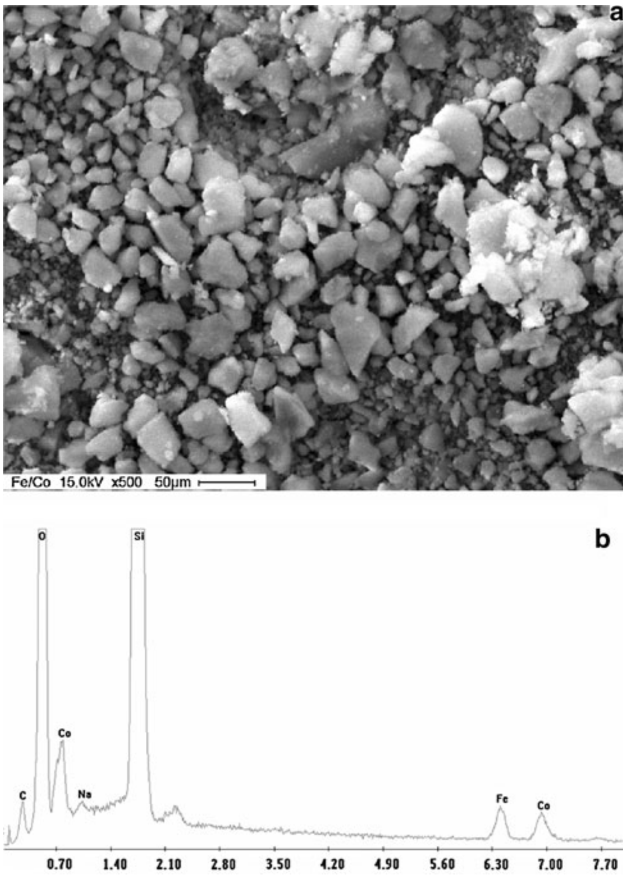

**Fig. 2** Scanning electron microscopy image (**a**) and corresponding chemical analysis results (**b**) of the FeCo–$SiO_2$ 10 wt% nanocomposite aerogel

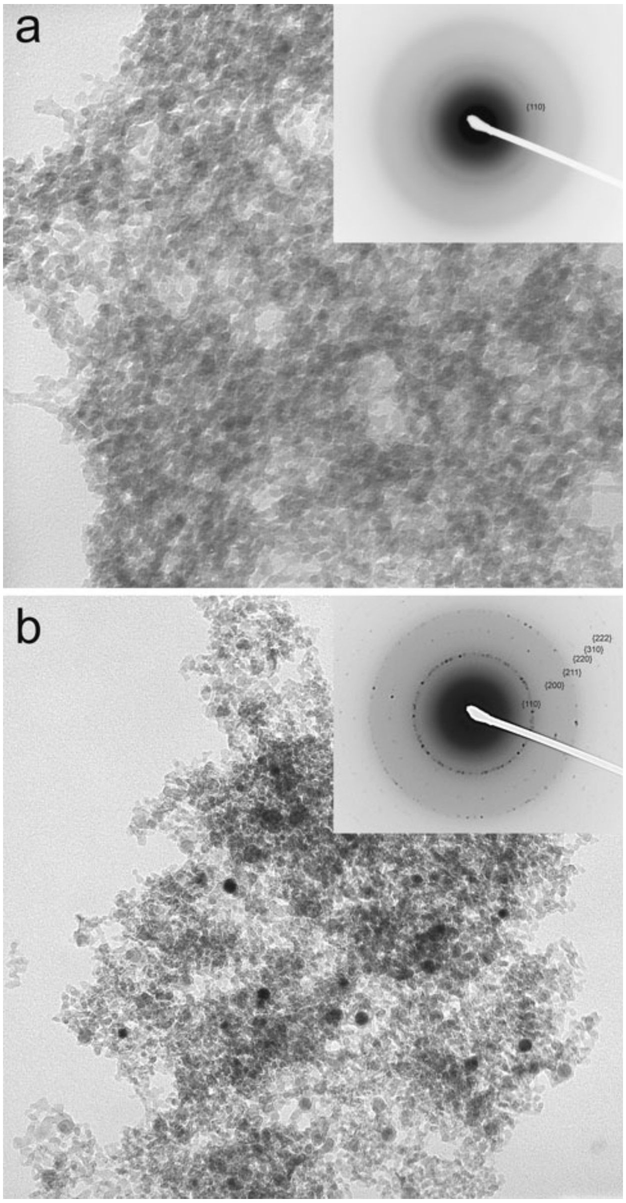

**Fig. 3** TEM images of the Fe of the FeCo–$SiO_2$ 5 wt% (**a**) and 10 wt% (**b**) nanocomposite aerogels and corresponding selected area electron diffraction (*inset*)

investigation clearly indicates that in both nanocomposites the silica network is highly branched, giving rise to the porous open structure typical of aerogels, with meso- and macropores.

The textural features of the nanocomposite catalysts such as the surface area, pore volume and pore size were further investigated by $N_2$ physisorption measurements at 77 K. The physisorption isotherms of the nanocomposites, shown in Fig. 4, are of type IV with an H1 hysteresis lying at high relative pressures, indicating the occurrence of interconnected mesopores with large size typical of the aerogel structure. In particular, the pore size is in the range 16–60 nm for both nanocomposites and the pore volume is 2.0 and 2.5 $cm^3/g$ for the 5 and 10 wt% catalysts, respectively. As pointed out previously the pore volumes derived by physisorption analysis only represent the lower value of the actual pore volumes [24, 25], the missing porosity being due to the occurrence of very large mesopores. The surface area varies from 274 to 314 $m^2/g$ going from the 5 to the 10 wt% composite. Physisorption data, in agreement with TEM investigation, indicate that the reduction treatment used to promote the formation of the FeCo alloy does not alter significantly the highly porous texture of the original aerogels. We ascribe the higher surface area and pore volume of the 10 wt% catalyst to the release of increasing amounts of precursor by products such as nitrogen oxide gasses (arising from the decomposition of metal nitrates during supercritical drying) which results in particular in a higher amount of micropores.

The FeCo–$SiO_2$ nanocomposite aerogels were tested as catalysts for the Fischer–Tropsch process. It should be pointed out that the aerogels prior to the reduction treatment, which results in the formation of the FeCo nanocrystals, are not catalytically active.

The catalytic results obtained with the FeCo–$SiO_2$ aerogels 10 wt% at different temperatures and $H_2$:CO ratios are reported in terms of CO conversion and selectivity in Fig. 5 and Table 2.

The aerogel is catalytically active already at 180 °C, where a relevant formation of condensable hydrocarbons is obtained. At 200 °C a high CO conversion and selectivity to $C_2$–$C_4$ fraction accompanied by a high production of $CO_2$ is observed. Further increase in temperature up to 220 °C results in a little increase in CO conversion.

Since, these data suggest that overall 200 °C is the most suitable temperature for the catalytic runs, then a $H_2$:CO ratio of 1.5:1 was also tested at this temperature, in order to reproduce reaction conditions close to biosyngas. As reported in Table 2, a decrease of the conversion is observed, indicating that this feed composition is detrimental. It is noteworthy that the catalytic behavior at all temperatures is reproducible, indicating that the aerogel is stable at the different temperatures tested.

The lower value of C balance can be ascribed to the formation of water soluble oxygenate by-products, favoured by lower $H_2$:CO molar ratio.

As a drawback, however, it should be pointed out that relatively high values of $CO_2$ and $CH_4$ selectivity, undesired for the development of clean energetic technologies are obtained at 200 °C.

The overall results of the catalytic test obtained with the 10 % loading aerogel are very promising compared to literature values of low temperature FT synthesis. In particular, a CO conversion of 14 and of 35 % has been recently obtained at 265 °C over an iron aerogel catalyst without

**Fig. 4** $N_2$ physisorption isotherms at 77 K and corresponding BJH pore size distribution as derived from the desorption branch (*inset*) for the FeCo–$SiO_2$ aerogel nanocomposites with an overall alloy loading of 5 wt% (*solid circles*) and 10 wt% (*empty squares*)

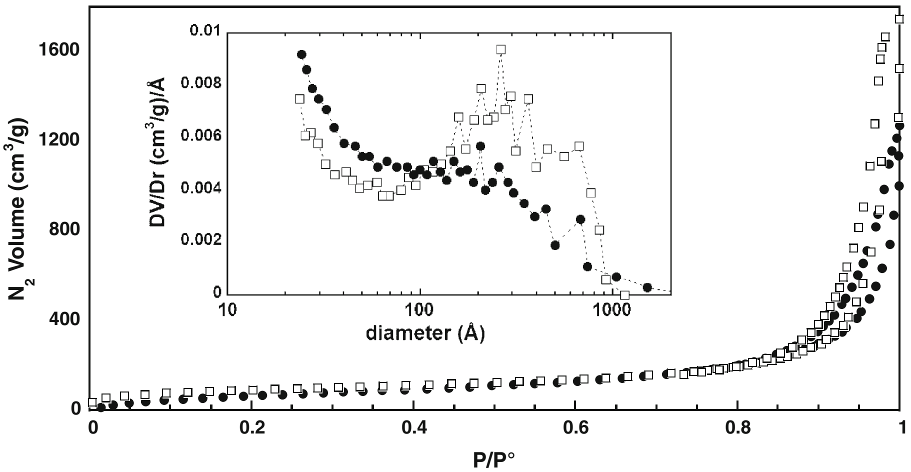

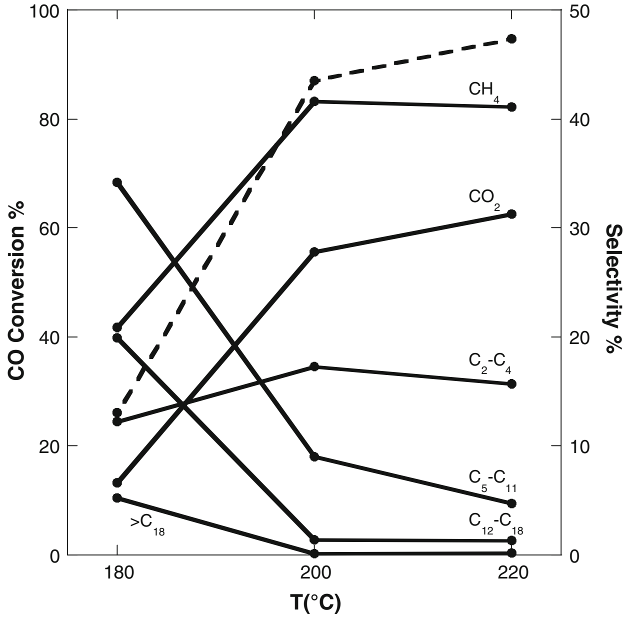

**Fig. 5** Selectivity (*solid lines*) and conversion (*dotted line*) of the FeCo–$SiO_2$ 10 wt% aerogel nanocomposite

and with doping with potassium (which acts as a promoter) respectively [26]. It was also shown that high yields of $C_2$ olefins are obtained and that the corresponding xerogel is less active (conversions of 7 %) [26]. Conversion of 22 % have been obtained at 265 °C by a catalyst made out of cobalt supported on silica which showed enhanced selectivity for $C_{9–10}$ [25]. Conversion values obtained on non aerogel catalysts having iron and cobalt as active phases reported in literature so far are even lower: for example, CO conversion of 2 % is obtained at 220 °C using different kind of iron–cobalt alloy systems supported on iron oxide spinel [8].

Moreover, FeCo–$SiO_2$ aerogel catalysts exhibited high stability. Protracted catalytic tests did not show any decrease in the catalytic activity of the nanocomposite aerogels even for long reaction times (72–96 h). For examples, the catalytic test performed at 200 °C showed CO conversion of 86.0 % after 48 h, 88.0 % after 72 h and 87.1 % after 80 h.

The FeCo–$SiO_2$ 5 wt% aerogel nanocomposite showed lower conversions than the 10 wt% catalyst. In particular,

**Table 2** Selectivity and conversion at different temperatures and $H_2$:CO ratio

| T (°C) | % Conversion (CO) | $H_2$:CO |
|---|---|---|
| 180 | 26.1 | 2:1 |
| 200 | 87.0 | 2:1 |
| 220 | 94.7 | 2:1 |
| 200 | 63.0 | 1.5:1 |

| T (°C) | Selectivity (%) | | | | | | C balance |
|---|---|---|---|---|---|---|---|
| | $CH_4$ | $CO_2$ | $C_2$–$C_4$ | $C_5$–$C_{11}$ (gasoline) | $C_{12}$–$C_{18}$ (diesel) | >$C_{18}$ (wax) | |
| 180 | 20.9 | 6.6 | 12.2 | 34.2 | 19.9 | 5.2 | 99.0 |
| 200 | 41.6 | 27.8 | 17.3 | 9.0 | 1.4 | <0.1 | 97.1 |
| 220 | 41.1 | 31.3 | 15.7 | 4.7 | 1.3 | 0.2 | 94.3 |
| 200 | 23.8 | 12.5 | 15.1 | 13.1 | 3.0 | 0.1 | 67.6 |

highest temperatures were required to obtain significant CO conversion values (around ~50 % for reaction temperatures up to 300 °C and rising to ~75 % at 320 °C). It is noteworthy, however, that likewise the catalyst with a higher alloy loading also this aerogel shows a high selectivity towards the formation of $C_2$–$C_4$ hydrocarbons.

The characterization by XRD, TEM and thermal analysis of the FeCo–$SiO_2$ 10 wt% catalyst after Fischer–Tropsch reaction is reported in the Supporting Information. The results indicate that the aerogel catalyst undergoes modification, giving rise to a denser structure containing a nanocrystalline phases. In particular, no evidence on the formation of carbides was obtained.

## 4 Conclusions

Nanocomposite aerogels made out of nanocrystalline iron–cobalt alloy dispersed on amorphous highly porous silica were tested as novel catalysts for the Fischer–Tropsch reaction.

The catalytic results indicate that the nanocomposite with a higher alloy loading (10 vs 5 wt%) exhibits an improved catalytic performance, giving rise to higher CO conversion values and being active at lower temperatures. In particular, the 5 wt% nanocomposite exhibits significant catalytic activity for reaction temperatures of 300 °C or higher. On the other hand, the 10 wt% FeCo–$SiO_2$ aerogel shows high thermal stability during the catalytic run and is active at relatively low temperatures (180 °C) with high CO conversion (87 %) already at 200 °C.

If we consider the yield of the gasoline ($C_5$–$C_{11}$ fraction) produced, the tests at 180 and 200 °C ($H_2$:CO = 2:1) give similar results, i.e. yields of 8.9 and 7.8 %, respectively. On the other hand, if we also take into account that the yield of $CO_2$ increases significantly with temperature (from 1.7 % at 180 °C to 24.2 % at 200 °C) the best reaction temperature for a clean production of gasoline using this catalyst is 180 °C, as in addition to the lower temperature offers the advantage of a very low production of $CO_2$ in front of a limited yield decrease.

In addition, the quite high selectivity for methane at high reaction temperatures, further supports that the catalyst is more promising at 180 °C.

Finally, the nanocomposite aerogel is highly selective towards the formation of $C_2$–$C_4$ hydrocarbons, indicating that these catalysts can be promising for the production of lower olefins by the Fischer–Tropsch synthesis.

**Acknowledgments** The Italian Institute of Technology (IIT) under the SEED project "NANOCAT" and Regione Autonoma della Sardegna through POR Sardegna FSE 2007–2013, L.R.7/2007 "Promozione della ricerca scientifica e dell'innovazione tecnologica in Sardegna" are gratefully acknowledged for financial support. The authors thank Dr. Alessandro Di Michele, Università di Perugia-Dipartimento di Fisica, for SEM analysis.

## References

1. de Klerk A (2011) Energy Environ Sci 4:1177–1205
2. Kamara BI, Coetzee J (2009) Energy Fuels 23:2242–2247
3. Schultz H (1999) Appl Catal. A 186:3–12
4. Jager B, Espinoza R (1995) Catal Today 23:17–28
5. Sie ST (1998) Rev Chem Eng 14:109–157
6. Duvenhage DJ, Covile NJ (2005) Appl Catal A 289:231–239
7. Tihay F, Pourroy G, Richard-Plouet M, Roger AC, Kiennemann A (2001) Appl Catal A 206:29–42
8. Cabet C, Roger AC, Kiennemann A, Lakamp S, Pourroy G (1998) J Catal 173:64–73
9. Davis BH (2007) Ind Eng Chem Res 46:8938–8945
10. O'Brien RJ, Xu L, Bao S, Raje A, Davis BH (2000) Appl Catal A 196:173–178
11. Rolison DR (2003) Science 299:1698–1701
12. Vallribera A, Molins E (2008) In: Astruc D (ed) Nanoparticles and catalysis. Wiley-VCH Verlag GmbH & Co. KGaA, Weinheim. doi:10.1002/9783527621323.ch5
13. Pajonk GM (1997) Cat Today 35:319–337
14. Ferino I, Casula MF, Corrias A, Cutrufello MG, Monaci R, Paschina G (2000) Phys Chem Chem Phys 2:1847–1854
15. Corrias A, Casula MF (2010) In: Aegerter M, Leventis N, Koebel M (eds) Aerogel handbook. Springer, New York, pp 335–363
16. Vanyorek L, Katona H, Loche D, Corrias A, Casula MF, Konya Z, Kukovecz A, Kiricsi I (2011) J Phys Chem C 115:5894–5902
17. Cutrufello MG, Rombi E, Ferino I, Loche D, Corrias A, Casula MF (2011) J Sol-Gel Sci Technol 60:324–332
18. Dunn BC, Cole P, Turpin GC, Ma Z, Pugmire RJ, Ernst RD, Eyring EM, Shah N, Huffman GP (2004) Prepr Pap-Am Chem Soc, Div Pet Chem 49:429–430
19. Casu A, Casula MF, Corrias A, Falqui A, Loche D, Marras S, Sangregorio C (2008) Phys Chem Chem Phys 10:1043–1052
20. Anderson RB (1956) In: Emmett PH (ed) Catalysts for the Fischer-Tropsch synthesis, vol 4 Van Nostrand Reinhold, New York, p 29
21. PDF-2 File, ICDD International Centre for Diffraction Data, 1601 Park Lane, Swarthmore, USA, card 44–1433
22. Carta D, Casula MF, Corrias A, Falqui A, Loche D, Mountjoy G, Wang P (2009) Chem Mater 21:945–953
23. Carta D, Mountjoy G, Gass M, Navarra G, Casula MF, Corrias A (2007) J Chem Phys 127:204705
24. Casula MF, Loche D, Marras S, Paschina G, Corrias A (2007) Langmuir 23:3509–3512
25. Dunn BC, Turpin GC, Cole P, Webster MC, Ma Z, Pugmire RJ, Ernst RD, Eyring EM, Shah N, Huffman GP (2004) Prepr Pap-Am Chem Soc, Div Pet Chem 49:431–434
26. Bali S, Huggins FE, Huffman GP, Ernst RD, Pugmire RJ, Eyring EM (2009) Energy Fuels 23:14–18